Efficient Monte Carlo simulation of spatio-temporal speckles and their correlations Supplementary material

CHEN BAR[1,*], IOANNIS GKIOULEKAS[2], AND ANAT LEVIN[1]

[1] *Department of Electrical and Computer Engineering, Technion, Haifa, Israel*
[2] *Robotics Institute, Carnegie Mellon University, PA, USA*
[*] *Corresponding author: chen.bar@campus.technion.ac.il*

This article provides supplement information to "Efficient Monte Carlo simulation of spatio-temporal speckles and their correlations". © 2023 Optical Society of America under the terms of the OSA Open Access Publishing Agreement

http://dx.doi.org/10.1364/optica.XX.XXXXXX

1. PATH-SPACE VIEW OF SPECKLE STATISTICS

Here we provide a detailed derivation for the speckle mean and covariance, expressing them as integrals in path space. These expressions are used in the main paper as the basis of the Monte Carlo rendering algorithms.

Fields as path sums. Our starting point is the classical theory of Twersky [1]: Given a scatterer configuration $O(t)$ and its temporal variation, we can approximate the solution to the Helmholtz equation as the sum of contributions over all paths $\vec{\mathbf{x}}(t)$ through $O(t)$. That is, consider the (enumerable) set $\mathbb{P}_{\mathbf{v}}^{\mathbf{i},O(t)}$ of all ordered sequences:

$$\vec{\mathbf{x}}(t) = \mathbf{o}_0(t) \to \ldots \to \mathbf{o}_{B+1}(t), \tag{S1}$$

with

$$\mathbf{o}_0(t) = \mathbf{i}, \ \mathbf{o}_{B+1}(t) = \mathbf{v}, \ \mathbf{o}_1(t), \ldots, \mathbf{o}_B(t) \in O(t), \tag{S2}$$

where $B = 0, \ldots, \infty$. In the notation $\vec{\mathbf{x}}(t)$ we assume that we can track the path over time. For example, $\vec{\mathbf{x}}(t_1), \vec{\mathbf{x}}(t_2)$ denote the position of the same particle sequence at two time instances.

Given the temporal set $O(t)$, the scattered field at each time instance can be expressed as

$$u_{\mathbf{v}}^{\mathbf{i},O}(t) = \sum_{\vec{\mathbf{x}}(t) \in \mathbb{P}(t)_{\mathbf{v}}^{\mathbf{i},O(t)}} \mu(\vec{\mathbf{x}}) \tag{S3}$$

$$= \sum_{\vec{\mathbf{x}}(t) \in \mathbb{P}_{\mathbf{v}}^{\mathbf{i},O(t)}} \mu(\mathbf{o}_0(t) \to \mathbf{o}_1(t)) \prod_{b=1}^{B} \mu(\mathbf{o}_{b-1}(t) \to \mathbf{o}_b(t) \to \mathbf{o}_{b+1}(t)).$$

Some paths are visualized in Fig. S1. The *complex-throughput* terms $\mu(\cdot)$ describe the amplitude and phase changes at each path segment, accounting for the scattering amplitude s and traveled length:

$$\mu(\mathbf{o}_{b-1}(t) \to \mathbf{o}_b(t) \to \mathbf{o}_{b+1}(t)) = \frac{1}{r(\mathbf{o}_b(t), \mathbf{o}_{b+1}(t))} \xi(\mathbf{o}_b(t) \to \mathbf{o}_{b+1}(t))$$
$$s(\widehat{\mathbf{o}_{b-1}(t)\mathbf{o}_b(t)} \cdot \widehat{\mathbf{o}_b(t)\mathbf{o}_{b+1}(t)}), \tag{S4}$$

$$\mu(\mathbf{o}_0(t) \to \mathbf{o}_1(t)) = \frac{1}{r(\mathbf{o}_0(t), \mathbf{o}_1(t))} \xi(\mathbf{o}_0(t) \to \mathbf{o}_1(t)). \tag{S5}$$

The *complex-transmission* terms $\xi(\cdot)$ account for phase change between path vertices $\mathbf{o}_b(t), \mathbf{o}_{b+1}(t)$, defined for points at the near field and far field, respectively, as

$$\xi(\mathbf{o}_b(t) \to \mathbf{o}_{b+1}(t)) = e^{ik|\mathbf{o}_b(t) - \mathbf{o}_{b+1}(t)|},$$
$$\xi(\hat{\mathbf{i}} \to \mathbf{o}(t)) = e^{ik(\hat{\mathbf{i}} \cdot \mathbf{o}(t))},$$
$$\xi(\mathbf{o}(t) \to \hat{\mathbf{v}}) = e^{-ik(\hat{\mathbf{v}} \cdot \mathbf{o}(t))}. \tag{S6}$$

and $1/r(\cdot)$ is the radial decay

$$r(\mathbf{o}_b(t), \mathbf{o}_{b+1}(t)) = |\mathbf{o}_b(t) - \mathbf{o}_{b+1}(t)|, \ r(\hat{\mathbf{i}}, \mathbf{o}(t)) = 1, \ r(\mathbf{o}(t), \hat{\mathbf{v}}) = 1. \tag{S7}$$

We note that for a fixed configuration $O(t)$ of scatterers, the complex transmission $\xi(\mathbf{o}_b(t) \to \mathbf{o}_{b+1}(t))$ is not attenuated as a function of the extinction coefficient. As we see below, volumetric attenuation comes into play only once we start averaging multiple random scatterer configurations.

Speckle statistics as path integrals. Using Eq. (S3), we can now express the mean by averaging over all particle configurations O that can be sampled from ς:

$$m_{\mathbf{v}}^{\mathbf{i}}(t) = \mathrm{E}_O \left[\sum_{\vec{\mathbf{x}}(t) \in \mathbb{P}(t)_{\mathbf{v}}^{\mathbf{i},O}} \mu(\vec{\mathbf{x}}(t)) \right]. \tag{S8}$$

Complex transmission:	$\xi(\mathbf{o}_b(t) \to \mathbf{o}_{b+1}(t)) = e^{ik|\mathbf{o}_b(t) - \mathbf{o}_{b+1}(t)|}$
Radial distance:	$r(\mathbf{o}_b(t), \mathbf{o}_{b+1}(t)) = |\mathbf{o}_b(t) - \mathbf{o}_{b+1}(t)|$
Scattering amplitude function:	$s(\widehat{\mathbf{o}_{b-1}(t)\mathbf{o}_b(t)} \cdot \widehat{\mathbf{o}_b(t)\mathbf{o}_{b+1}(t)})$
Complex throughput:	$\mu(\mathbf{o}_{b-1}(t) \to \mathbf{o}_b(t) \to \mathbf{o}_{b+1}(t)) = \frac{1}{r(\mathbf{o}_b(t),\mathbf{o}_{b+1}(t))} \xi(\mathbf{o}_b(t) \to \mathbf{o}_{b+1}(t)) s(\widehat{\mathbf{o}_{b-1}(t)\mathbf{o}_b(t)} \cdot \widehat{\mathbf{o}_b(t)\mathbf{o}_{b+1}(t)})$
Volumetric attenuation:	$\alpha(\mathbf{o}_b(t), \mathbf{o}_{b+1}(t)) = e^{-\frac{1}{2}\int_0^1 \sigma_t(\beta\mathbf{o}_b(t) + (1-\beta)\mathbf{o}_{b+1}(t))\,d\beta}$
Attenuation + radial decay:	$\tilde{\alpha}(\mathbf{o}_b(t), \mathbf{o}_{b+1}(t)) = \frac{1}{r(\mathbf{o}_b(t),\mathbf{o}_{b+1}(t))} \alpha(\mathbf{o}_b(t), \mathbf{o}_{b+1}(t))$
Complex volumetric throughput:	$v(\mathbf{o}_{b-1}(t) \to \mathbf{o}_b(t) \to \mathbf{o}_{b+1}(t)) = \alpha(\mathbf{o}_b(t), \mathbf{o}_{b+1}(t)) \mu(\mathbf{o}_{b-1}(t) \to \mathbf{o}_b(t) \to \mathbf{o}_{b+1}(t))$
Momentum transfer:	$\gamma(\widehat{\mathbf{o}_b\mathbf{o}_{b+1}} - \widehat{\mathbf{o}_{b-1}\mathbf{o}_b}) = e^{-k^2 D|t| \|\widehat{\mathbf{o}_b\mathbf{o}_{b+1}} - \widehat{\mathbf{o}_{b-1}\mathbf{o}_b}\|^2 + ikt(\widehat{\mathbf{o}_b\mathbf{o}_{b+1}} - \widehat{\mathbf{o}_{b-1}\mathbf{o}_b}) \cdot \mathbf{U}}$

Table S1. Types of path contributions. Summary of notation and relationships between different throughput terms used in our Monte Carlo algorithms.
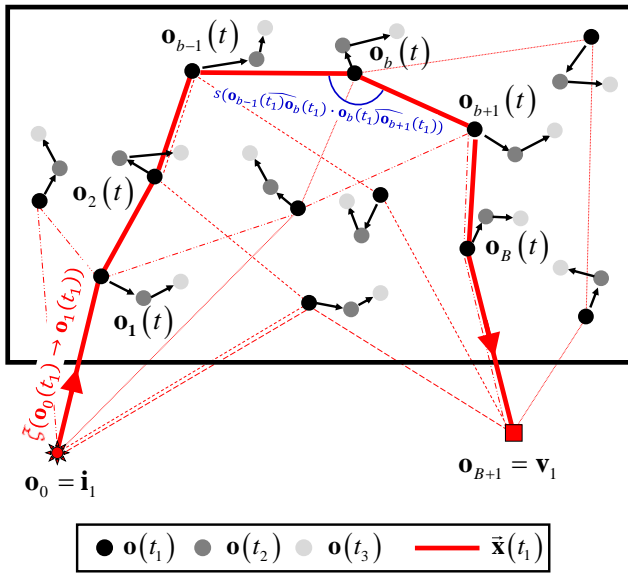
Fig. S1. The Twersky's approximation: Given a scatterer instantiation O, the speckle field can be approximated as a sum of complex contributions over *all* paths. The path contribution encapsulates its length and scattering events along the path.

To simplify notation, we assume particle density is stationary over time. Thus we can neglect the time index and denote $m_{\mathbf{v}}^{\mathbf{i}}$.

To define the temporal covariance we consider pairs of paths $(\vec{\mathbf{x}}^1(t))$, $(\vec{\mathbf{x}}^2(t))$ through the *same* particle instantiation $O(t)$, at two different times.

The speckle field for each particle configuration is an average of complex throughput as in Eq. (S3), hence, by combining Eq. (7) of the main paper with Eq. (S3) the covariance is obtained by averaging these over all moving particle configurations sampled from the bulk material densities:

$$C_{\mathbf{v}_1,\mathbf{v}_2}^{\mathbf{i}_1,\mathbf{i}_2}(t_1,t_2) = E_O \left[\sum_{\substack{\vec{\mathbf{x}}^1(t_1) \in \mathbb{P}_{\mathbf{v}_1}^{\mathbf{i}_1,O(t_1)}, \\ \vec{\mathbf{x}}^2(t_2) \in \mathbb{P}_{\mathbf{v}_2}^{\mathbf{i}_2,O(t_2)}}} \mu(\vec{\mathbf{x}}^1(t_1)) \cdot \mu(\vec{\mathbf{x}}^2(t_2))^* \right]$$
$$- m_{\mathbf{v}_1}^{\mathbf{i}_1} \cdot m_{\mathbf{v}_2}^{\mathbf{i}_2*}. \tag{S9}$$

By exchanging the order of expectation and summation in

Eq. (S8) and Eq. (S9), we have:

$$m_{\mathbf{v}}^{\mathbf{i}} = \int_{\mathbb{P}_{\mathbf{v}}^{\mathbf{i}}} p(\vec{\mathbf{x}}) \mu(\vec{\mathbf{x}})\, d\vec{\mathbf{x}}, \tag{S10}$$

$$C_{\mathbf{v}_1,\mathbf{v}_2}^{\mathbf{i}_1,\mathbf{i}_2}(t_1,t_2) = \iint_{\mathbb{P}_{\mathbf{v}_1}^{\mathbf{i}_1,t_1}, \mathbb{P}_{\mathbf{v}_2}^{\mathbf{i}_2,t_2}} c_{\vec{\mathbf{x}}^1,\vec{\mathbf{x}}^2}(t_1,t_2)\, d\vec{\mathbf{x}}^1(t_1)\, d\vec{\mathbf{x}}^2(t_2)$$
$$- m_{\mathbf{v}_1}^{\mathbf{i}_1} m_{\mathbf{v}_2}^{\mathbf{i}_2*}, \tag{S11}$$

with

$$c_{\vec{\mathbf{x}}^1,\vec{\mathbf{x}}^2}(t_1,t_2) = p(\vec{\mathbf{x}}^1(t_1), \vec{\mathbf{x}}^2(t_2)) \cdot \mu(\vec{\mathbf{x}}^1(t_1)) \cdot \mu(\vec{\mathbf{x}}^2(t_2))^*, \tag{S12}$$

where now the space $\mathbb{P}_{\mathbf{v}}^{\mathbf{i},t}$ includes paths with vertices $\mathbf{o}_1(t), \ldots, \mathbf{o}_B(t)$ that can be *anywhere* in the volume $\mathcal{V}$ at time t, not only on fixed particle locations. Unlike $\mathbb{P}_{\mathbf{v}}^{\mathbf{i},O(t)}$, $\mathbb{P}_{\mathbf{v}}^{\mathbf{i},t}$ is not an enumerable space, thus summation is replaced with integration. Each path sequence follows displacement sequences $\vec{\Delta}_{t_2-t_1}^1 = \vec{\mathbf{x}}^1(t_2) - \vec{\mathbf{x}}^1(t_1)$ and $\vec{\Delta}_{t_2-t_1}^2 = \vec{\mathbf{x}}^2(t_2) - \vec{\mathbf{x}}^2(t_1)$. The term $p(\vec{\mathbf{x}}^1(t_1), \vec{\mathbf{x}}^2(t_2))$ is the probability that all vertices on both $\vec{\mathbf{x}}^1(t_1)$, $\vec{\mathbf{x}}^2(t_2)$ are included in the *same* sampled particle configuration O at two different time instances, and their displacements $\vec{\Delta}_{t_2-t_1}^1$, $\vec{\Delta}_{t_2-t_1}^2$ come from the motion distribution $\mathcal{T}$.

In the following sections, we show that $m_{\mathbf{v}}^{\mathbf{i}}$ can be computed in closed form, and we greatly simplify the path integral for $C_{\mathbf{v}_1,\mathbf{v}_2}^{\mathbf{i}_1,\mathbf{i}_2}(t_1,t_2)$ by characterizing the pairs of paths that have non-zero contributions.

A. The speckle mean

Evaluating the speckle mean is addressed by standard textbooks on scattering [2, 3]. We present these results here.

We consider a source at $\mathbf{o}_1$. As this wave scatters, we want to evaluate the average contribution of all paths $\vec{\mathbf{x}}$ starting at $\mathbf{o}_1$ and arriving at a second point $\mathbf{o}_2$. As derived in [3], the averages can be expressed analytically as

$$\int_{\mathbb{P}_{\mathbf{o}_1}^{\mathbf{o}_2}} p(\vec{\mathbf{x}}) \mu(\vec{\mathbf{x}})\, d\vec{\mathbf{x}} = \alpha(\mathbf{o}_1, \mathbf{o}_2) \cdot \mu(\mathbf{o}_1 \to \mathbf{o}_2), \tag{S13}$$

where μ is defined as in Eq. (S4). The *volumetric attenuation* α is the probability of getting from $\mathbf{o}_1$ to $\mathbf{o}_2$ without encountering other particles, and equals for the near-field and far-field cases, respectively:

$$\alpha(\mathbf{o}_1, \mathbf{o}_2) = e^{-\frac{1}{2}\int_0^1 \sigma_t(\beta\mathbf{o}_1 + (1-\beta)\mathbf{o}_2)\, d\beta},$$
$$\alpha(\hat{\mathbf{i}}, \mathbf{o}) = e^{-\frac{1}{2}\int_0^\infty \sigma_t(\mathbf{o}_1 - \beta\hat{\mathbf{i}})\, d\beta}. \tag{S14}$$
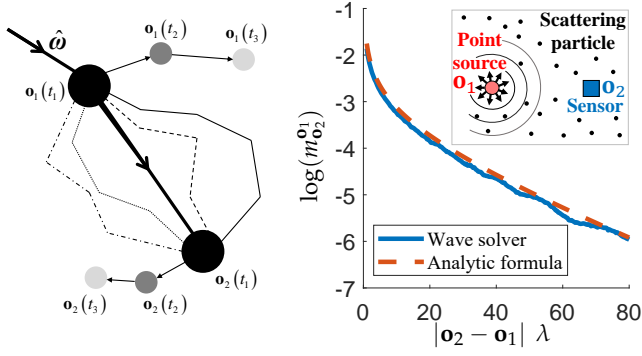
Fig. S2. Paths for speckle mean. (a) The average contribution of all paths connecting $\mathbf{o}_1$ and $\mathbf{o}_2$ (dashed lines) reduces to the contribution of the direct path (solid line). (b) We numerically simulate the speckle mean for the setup in the inset. We sample multiple particle configurations, use a wave equation solver to compute the field scattered from a source at point $\mathbf{o}_1$ to a sensor at point $\mathbf{o}_2$, and average the solutions. The empirical mean of the scattered fields agrees with the speckle mean computed using Eq. (S13).

For a homogeneous medium, $\alpha(\mathbf{o}_1, \mathbf{o}_2) = \exp(-\frac{1}{2}\sigma_t|\mathbf{o}_2 - \mathbf{o}_1|)$. The factor $1/2$ in the exponent of Eq. (S14) makes α the square root of the volumetric attenuation term in standard radiative transfer. Intuitively, this is because we deal with the field rather than intensity.

The main intuition behind Eq. (S13) is that, as most paths contribute essentially random complex phases, they cancel each other out. Therefore, the total field from $\mathbf{o}_1$ to $\mathbf{o}_2$ equals the field that travels only along the *direct path* between the two points, attenuated by the exponentially decaying probability $\alpha(\mathbf{o}_1, \mathbf{o}_2)$, see Fig. S2(a). This exponential decay is the result of the phase cancellations between many paths.

In particular, the speckle mean $m_\mathbf{v}^\mathbf{i}$ of Eq. (S10) is

$$m_\mathbf{v}^\mathbf{i} = \alpha(\mathbf{i}, \mathbf{v}) \cdot \mu(\mathbf{i} \rightarrow \mathbf{v}). \tag{S15}$$

The main consequence of this section is that computing the speckle mean becomes a *direct illumination* problem, which can be solved analytically without the need for path integration. In Fig. S2(b), we numerically evaluate the speckle mean by averaging multiple solutions of the wave equation as in Eq. (4) of the main paper, showing a good agreement with the analytic formula of Eq. (S15). We note that, as the speckle mean decays exponentially with the distance, in most cases it is negligible, making the computation of covariance the main challenge in simulating speckle. We discuss this next.

B. The speckle covariance

We have shown in Eq. (S11) that the speckle covariance can be expressed as an integral over *pairs* of paths $\vec{\mathbf{x}}^1(t_1)$ from $\mathbf{i}_1$ to $\mathbf{v}_1$ at time t_1 and $\vec{\mathbf{x}}^2(t_2)$ from $\mathbf{i}_2$ to $\mathbf{v}_2$ at time t_2. Unlike the mean, there is no closed-form expression for this integral. However, we can considerably simplify Eq. (S11) by characterizing the pairs of paths $\vec{\mathbf{x}}^1, \vec{\mathbf{x}}^2$ for which its integrand $c_{\vec{\mathbf{x}}^1, \vec{\mathbf{x}}^2}(t_1, t_2)$ is non-zero, as well as deriving a simple formula for $c_{\vec{\mathbf{x}}^1, \vec{\mathbf{x}}^2}(t_1, t_2)$ for those pairs. Some of the arguments we use are discussed in Mishchenko *et al.* [3]. Our end result is a path-integral expression for covariance that lends itself to Monte Carlo integration.

For ease of notation, w.l.o.g. we consider two time instances of the form $t_1 = -t/2$, $t_2 = t/2$. We denote the mean particle
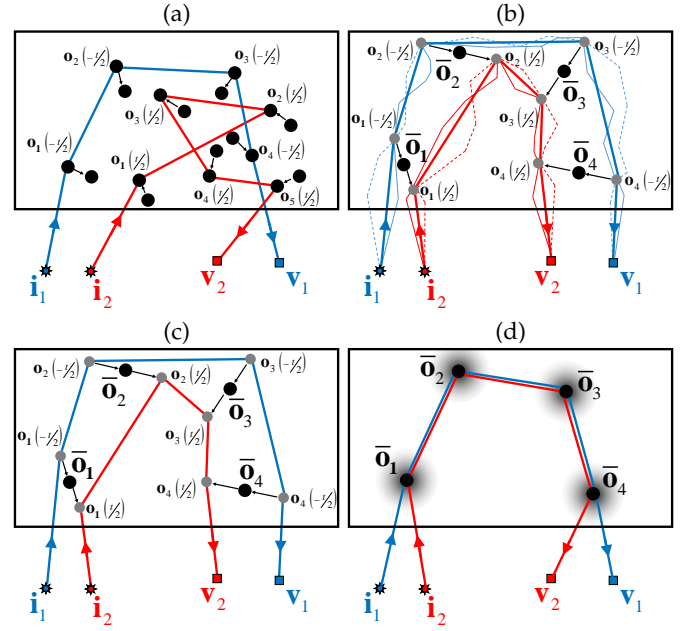
Fig. S3. Path pairs for speckle covariance: (a) A naive approach for computing speckle covariance would sum path contributions over all pairs of paths from $\mathbf{i}_1$ to $\mathbf{v}_1$ and from $\mathbf{i}_2$ to $\mathbf{v}_2$. However most such paths have random phases and do not contribute to the correlation. (b) Path segments between nodes $\mathbf{o}_b, \mathbf{o}_{b+1}$ on path $\vec{\mathbf{x}}^1$, which are not shared by path $\vec{\mathbf{x}}^2$, and vice versa. It can be proved that all such path segments average to the direct path from $\mathbf{o}_b$ to $\mathbf{o}_{b+1}$. (c) As a result, the path integral can be reduced to consider only path pairs sharing all their nodes. Note that if we are computing correlations at two different time instances t_1, t_2, the path $\vec{\mathbf{x}}^1$ traces the position of the scatterer at time instance t_1 and the path $\vec{\mathbf{x}}^2$ traces its position at time t_2. (d) We can further simplify the covariance estimate and consider only the mean paths, so the path pairs perfectly share all their central segments. Around each node in the path we analytically integrate the contribution of all possible motions.

position by

$$\bar{\mathbf{o}} = \frac{1}{2}\left(\mathbf{o}(t_1) + \mathbf{o}(t_2)\right), \tag{S16}$$

so that $\mathbf{o}(t_1) = \bar{\mathbf{o}} - 1/2\boldsymbol{\Delta_t}$, $\mathbf{o}(t_2) = \bar{\mathbf{o}} + 1/2\boldsymbol{\Delta_t}$.

Valid pairs of paths. Intuitively the covariance is not affected by independent path pairs $\vec{\mathbf{x}}^1(t_1), \vec{\mathbf{x}}^2(t_2)$, and hence, as derived below, the dependent path pairs we need to consider in practice are only the ones sharing their vertices.

Consider, as in Fig. S3(b), the set of path pairs $\vec{\mathbf{x}}^1(t), \vec{\mathbf{x}}^2(t)$ that have an arbitrary number of vertices, but share only vertices $\mathbf{o}_1, \ldots, \mathbf{o}_B$. Then, as in Sec. A, we expect all the different path segments from $\mathbf{o}_b$ to $\mathbf{o}_{b+1}$ to average to the direct path between these points. Mishchenko *et al.* [3] prove that indeed all path pairs with disjoint vertices collapse to their joint vertices, and the covariance integral can reduce to the family of path pairs sharing all their vertices, as in Fig. S3(c). To formulate this argument we consider the space $\mathbb{P}(t)$ of *sub-paths* $\vec{\mathbf{x}}^s = \bar{\mathbf{o}}_1 \rightarrow \cdots \rightarrow \bar{\mathbf{o}}_B$, and displacements $\vec{\boldsymbol{\Delta}}_t = \boldsymbol{\Delta_{t1}}, \ldots, \boldsymbol{\Delta_{tB}}$ where $B = 1, \ldots, \infty$, and each vertex $\bar{\mathbf{o}}$ can be everywhere in $\mathcal{V}$. We can evaluate the covariance

integral of Eq. (S11) by considering only path pairs of the form:

$$\vec{\mathbf{x}}^1\left(-\tfrac{t}{2}\right) = \mathbf{i}_1 \to \vec{\mathbf{x}}^s - 1/2\vec{\boldsymbol{\Delta}}_t \to \mathbf{v}_1,$$
$$\vec{\mathbf{x}}^2\left(\tfrac{t}{2}\right) = \mathbf{i}_2 \to \vec{\mathbf{x}}^s + 1/2\vec{\boldsymbol{\Delta}}_t \to \mathbf{v}_2. \tag{S17}$$

Claim S1 *The covariance integral of* Eq. (S11) *can be evaluated using only joint path pairs*

$$C_{\mathbf{v}_1,\mathbf{v}_2}^{\mathbf{i}_1,\mathbf{i}_2}\left(-\tfrac{t}{2},\tfrac{t}{2}\right) = \iint_{\mathbb{P}(t)} c_{\vec{\mathbf{x}}^s,\vec{\boldsymbol{\Delta}}_t}\left(-\tfrac{t}{2},\tfrac{t}{2}\right)\,\mathrm{d}\vec{\boldsymbol{\Delta}}_t\,\mathrm{d}\vec{\mathbf{x}}^s, \tag{S18}$$

where the average contribution of all pairs of paths sharing vertices $\mathbf{o}_1,\dots,\mathbf{o}_B$ *is*

$$c_{\vec{\mathbf{x}}^s,\vec{\boldsymbol{\Delta}}_t}\left(-\tfrac{t}{2},\tfrac{t}{2}\right) = \prod_{b=0}^{B} f_b, \tag{S19}$$

and

$$
f_b = \begin{cases}
v(\mathbf{i}_1 \to \mathbf{o}_1(-\tfrac{t}{2}))v(\mathbf{i}_2 \to \mathbf{o}_1(\tfrac{t}{2}))^*, & \text{for } b = 0 \\[2ex]
p(\boldsymbol{\Delta}_{\mathbf{t}b})\sigma_s(\bar{\mathbf{o}}_{b+1})v(\mathbf{o}_{b-1}(-\tfrac{t}{2}) \to \mathbf{o}_b(-\tfrac{t}{2}) \to \mathbf{o}_{b+1}(-\tfrac{t}{2}))\cdot \\
v(\mathbf{o}_{b-1}(\tfrac{t}{2}) \to \mathbf{o}_b(\tfrac{t}{2}) \to \mathbf{o}_{b+1}(\tfrac{t}{2}))^*, & \text{for } 1 \le b \le B-1 \\[2ex]
p(\boldsymbol{\Delta}_{\mathbf{t}B})v(\mathbf{o}_{B-1}(-\tfrac{t}{2}) \to \mathbf{o}_B(-\tfrac{t}{2}) \to \mathbf{v}_1)\cdot \\
v(\mathbf{o}_{B-1}(\tfrac{t}{2}) \to \mathbf{o}_B(\tfrac{t}{2}) \to \mathbf{v}_2)^*, & \text{for } b = B
\end{cases}
\tag{S20}
$$

with

$$v(\mathbf{o}_{b-1}(t) \to \mathbf{o}_b(t) \to \mathbf{o}_{b+1}(t)) = \alpha(\mathbf{o}_b(t),\mathbf{o}_{b+1}(t))$$
$$\cdot\,\mu(\mathbf{o}_{b-1}(t) \to \mathbf{o}_b(t) \to \mathbf{o}_{b+1}(t)), \tag{S21}$$

$$v(\mathbf{o}_0(t) \to \mathbf{o}_1(t)) = \alpha(\mathbf{o}_0(t),\mathbf{o}_1(t)) \cdot \mu(\mathbf{o}_0(t) \to \mathbf{o}_1(t)). \tag{S22}$$

The proof can be found in [3] and we do not review it here. We note however, that the integral considers only subpaths of length $B \ge 1$ that have scattered in at least one particle. We neglect direct paths of length $B = 0$ as those are directly equivalent to the mean $m_{\mathbf{v}_1}^{\mathbf{i}_1} m_{\mathbf{v}_2}^{\mathbf{i}_2}$, which is subtracted in Eq. (S11).

To compare the integral in Eq. (S18) to the original integral in Eq. (S11) we note that when all path pairs are included the path contribution is the complex throughput $\mu(\cdot)$ of Eq. (S4) and Eq. (S5). In the above claim only joint path pairs are considered, but the complex throughput $\mu(\cdot)$ is replaced by the *complex volumetric throughput* term $v(\cdot)$, which multiplies the complex throughput with the volumetric attenuation of Eq. (S14). This exponential attenuation is a result of integration over the space of disjoint path segments.

To recap, the complex volumetric throughput is the product of these factors: (i) the radial decay (ii) the volumetric attenuation α; (iii) the complex transmission ξ, whose phase is proportional to the path segment length; and (iv) the scattering amplitude function s due a change of direction (for paths with $B > 1$). For example:

$$v(\mathbf{o}_{b-1}(t) \to \mathbf{o}_b(t) \to \mathbf{o}_{b+1}(t)) = \frac{1}{r(\mathbf{o}_b(t),\mathbf{o}_{b+1}(t))}\alpha(\mathbf{o}_b(t),\mathbf{o}_{b+1}(t))\cdot$$
$$\xi(\mathbf{o}_b(t) \to \mathbf{o}_{b+1}(t))s(\widehat{\mathbf{o}_{b-1}(t)\mathbf{o}_b(t)} \cdot \widehat{\mathbf{o}_b(t)\mathbf{o}_{b+1}(t)}) \tag{S23}$$

The different terms are summarized in Table S1.

The contribution of joint path pairs, given by Eq. (S19), is Markovian and can be computed analytically. When $t_1 = t_2$

the paths $\vec{\mathbf{x}}^1(t_1)$, $\vec{\mathbf{x}}^2(t_2)$ share all their central segments and the formula simplifies considerably. In particular, the lengths of the central segments $1 \le b \le B-1$ on both paths are equal and so is their phase

$$\xi(\mathbf{o}_b(-\tfrac{t}{2}) \to \mathbf{o}_{b+1}(-\tfrac{t}{2})) = \xi(\mathbf{o}_b(\tfrac{t}{2}) \to \mathbf{o}_{b+1}(\tfrac{t}{2})), \tag{S24}$$

hence

$$v(\mathbf{o}_{b-1}(-\tfrac{t}{2}) \to \mathbf{o}_b(-\tfrac{t}{2}) \to \mathbf{o}_{b+1}(-\tfrac{t}{2}))\cdot$$
$$v(\mathbf{o}_{b-1}(\tfrac{t}{2}) \to \mathbf{o}_b(\tfrac{t}{2}) \to \mathbf{o}_{b+1}(\tfrac{t}{2}))^* \tag{S25}$$

is a positive real number with no imaginary part, rather than a complex number.

In the general case, however, we are interested in correlations at two different time instances, in which case the pairwise path contribution $c_{\vec{\mathbf{x}}^s,\vec{\boldsymbol{\Delta}}_t}\left(-\tfrac{t}{2},\tfrac{t}{2}\right)$, is complex. We can still simplify Eq. (S20) considerably as described next. First, we assume that the particle motion is considerably lower than the mean free path (the average distance between successive particles on a path). In this case, to a first order approximation:

$$\alpha(\mathbf{o}_b(-\tfrac{t}{2}),\mathbf{o}_{b+1}(-\tfrac{t}{2})) \approx \alpha(\mathbf{o}_b(\tfrac{t}{2}),\mathbf{o}_{b+1}(\tfrac{t}{2})), \tag{S26}$$
$$r(\mathbf{o}_b(-\tfrac{t}{2}),\mathbf{o}_{b+1}(-\tfrac{t}{2})) \approx r(\mathbf{o}_b(\tfrac{t}{2}),\mathbf{o}_{b+1}(\tfrac{t}{2})), \tag{S27}$$

for $0 \le b \le B$, and:

$$s(\widehat{\mathbf{o}_{b-1}(-\tfrac{t}{2})\,\mathbf{o}_b}(-\tfrac{t}{2}) \cdot \mathbf{o}_b\widehat{(-\tfrac{t}{2})\,\mathbf{o}_{b+1}}(-\tfrac{t}{2})) \approx$$
$$s(\widehat{\mathbf{o}_{b-1}(\tfrac{t}{2})\,\mathbf{o}_b}(\tfrac{t}{2}) \cdot \mathbf{o}_b\widehat{(\tfrac{t}{2})\,\mathbf{o}_{b+1}}(\tfrac{t}{2})) \tag{S28}$$

for $1 \le b \le B$, where at the end nodes we plug $\mathbf{o}_0(-\tfrac{t}{2}) = \mathbf{i}_1$, $\mathbf{o}_0(\tfrac{t}{2}) = \mathbf{i}_2$, $\mathbf{o}_{B+1}(-\tfrac{t}{2}) = \mathbf{v}_1$, $\mathbf{o}_{B+1}(\tfrac{t}{2}) = \mathbf{v}_2$. For directional sources and sensors, $\widehat{\mathbf{i}\mathbf{o}_1}$ is just the direction $\hat{\mathbf{i}}$.

The complex transmission ξ cannot be dismissed, as phase differences between the paths are the main cause for the reduction in correlation. We can still approximate the phase difference in a simpler way, summarized in the following claim.

Claim S2 *The complex transmission ξ of paths sharing their central segments can be approximated as*

$$\prod_{b=0}^{B} \xi(\mathbf{o}_b(-\tfrac{t}{2}) \to \mathbf{o}_{b+1}(-\tfrac{t}{2})) \cdot \xi(\mathbf{o}_b(\tfrac{t}{2}) \to \mathbf{o}_{b+1}(\tfrac{t}{2}))^* \approx$$
$$\prod_{b=1}^{B} e^{ik(\widehat{\bar{\mathbf{o}}_b\bar{\mathbf{o}}_{b+1}} - \widehat{\bar{\mathbf{o}}_{b-1}\bar{\mathbf{o}}_b})\cdot\boldsymbol{\Delta}_{\mathbf{t}b}}, \tag{S29}$$

where for the start and end nodes we plug above $\bar{\mathbf{o}}_0 = 1/2(\mathbf{i}_1 + \mathbf{i}_2)$ *and* $\bar{\mathbf{o}}_{B+1} = 1/2(\mathbf{v}_1 + \mathbf{v}_2)$.

Proof: Since the mean particle motion is considerably lower than the mean free path, we estimate for $1 \le b \le B-1$

$$\xi(\mathbf{o}_b(-\tfrac{t}{2}) \to \mathbf{o}_{b+1}(-\tfrac{t}{2})) \cdot \xi(\mathbf{o}_b(\tfrac{t}{2}) \to \mathbf{o}_{b+1}(\tfrac{t}{2}))^* =$$
$$e^{ik\left(\left|\mathbf{o}_b(-\tfrac{t}{2}) - \mathbf{o}_{b+1}(-\tfrac{t}{2})\right| - \left|\mathbf{o}_b(\tfrac{t}{2}) - \mathbf{o}_{b+1}(\tfrac{t}{2})\right|\right)} \approx$$
$$e^{ik\left(\left(\mathbf{o}_{b+1}(-\tfrac{t}{2}) - \mathbf{o}_b(-\tfrac{t}{2})\right)\widehat{\bar{\mathbf{o}}_b\bar{\mathbf{o}}_{b+1}} - \left(\mathbf{o}_{b+1}(\tfrac{t}{2}) - \mathbf{o}_b(\tfrac{t}{2})\right)\widehat{\bar{\mathbf{o}}_b\bar{\mathbf{o}}_{b+1}}\right)} =$$
$$e^{ik\left((\boldsymbol{\Delta}_{\mathbf{t}b} - \boldsymbol{\Delta}_{\mathbf{t}b+1})\widehat{\bar{\mathbf{o}}_b\bar{\mathbf{o}}_{b+1}}\right)}, \tag{S30}$$

for $b = 0$ and for point sources

$$\xi(\mathbf{o}_0\left(-\tfrac{t}{2}\right)\!\to\!\mathbf{o}_1\left(-\tfrac{t}{2}\right)) \cdot \xi(\mathbf{o}_0\left(\tfrac{t}{2}\right)\!\to\!\mathbf{o}_1\left(\tfrac{t}{2}\right))^* =$$

$$e^{ik\left(\left|\mathbf{i}_1-\mathbf{o}_1\left(-\frac{t}{2}\right)\right|-\left|\mathbf{i}_2-\mathbf{o}_1\left(\frac{t}{2}\right)\right|\right)} \approx$$

$$e^{ik\left(\left(\mathbf{o}_1\left(-\frac{t}{2}\right)-\mathbf{i}_1\right)\widehat{\mathbf{i}_1\mathbf{o}_1}-\left(\mathbf{o}_1\left(\frac{t}{2}\right)-\mathbf{i}_2\right)\widehat{\mathbf{i}_2\mathbf{o}_1}\right)} =$$

$$e^{ik\left((\mathbf{i}_1-\bar{\mathbf{o}}_1)\widehat{\mathbf{i}_1\bar{\mathbf{o}}_1}-(\mathbf{i}_2-\bar{\mathbf{o}}_1)\widehat{\mathbf{i}_2\bar{\mathbf{o}}_1}-0.5\Delta_{\mathbf{t}1}\left(\widehat{\mathbf{i}_1\bar{\mathbf{o}}_1}+\widehat{\mathbf{i}_2\bar{\mathbf{o}}_1}\right)\right)} =$$

$$e^{ik\left(\left|\mathbf{i}_1-\bar{\mathbf{o}}_1\right|-\left|\mathbf{i}_2-\bar{\mathbf{o}}_1\right|-0.5\Delta_{\mathbf{t}1}\left(\widehat{\mathbf{i}_1\bar{\mathbf{o}}_1}+\widehat{\mathbf{i}_2\bar{\mathbf{o}}_1}\right)\right)} \approx$$

$$\xi(\mathbf{o}_0\left(-\tfrac{t}{2}\right)\!\to\!\bar{\mathbf{o}}_1) \cdot \xi(\mathbf{o}_0\left(\tfrac{t}{2}\right)\!\to\!\bar{\mathbf{o}}_1)^* e^{-ik\cdot\Delta_{\mathbf{t}1}\cdot\widehat{\frac{\mathbf{i}_1+\mathbf{i}_2}{2}\bar{\mathbf{o}}_1}}, \qquad (S31)$$

and for directional sources

$$e^{ik\left(\hat{\mathbf{i}}_1\cdot\mathbf{o}_1\left(-\frac{t}{2}\right)-\hat{\mathbf{i}}_2\cdot\mathbf{o}_1\left(\frac{t}{2}\right)\right)} =$$

$$e^{ik\left(\hat{\mathbf{i}}_1\cdot(\bar{\mathbf{o}}_1-0.5\Delta_{\mathbf{t}1})-\hat{\mathbf{i}}_2\cdot(\bar{\mathbf{o}}_1+0.5\Delta_{\mathbf{t}1})\right)} =$$

$$\xi(\mathbf{o}_0\left(-\tfrac{t}{2}\right)\!\to\!\bar{\mathbf{o}}_1) \cdot \xi(\mathbf{o}_0\left(\tfrac{t}{2}\right)\!\to\!\bar{\mathbf{o}}_1)^* e^{-ik\cdot\Delta_{\mathbf{t}1}\cdot\frac{\hat{\mathbf{i}}_1+\hat{\mathbf{i}}_2}{2}}. \qquad (S32)$$

Similarly for $b = B$

$$\xi(\mathbf{o}_B\left(-\tfrac{t}{2}\right)\!\to\!\mathbf{o}_{B+1}\left(-\tfrac{t}{2}\right)) \cdot \xi(\mathbf{o}_B\left(\tfrac{t}{2}\right)\!\to\!\mathbf{o}_{B+1}\left(\tfrac{t}{2}\right))^* \approx$$

$$\xi(\bar{\mathbf{o}}_B\!\to\!\mathbf{o}_{B+1}\left(-\tfrac{t}{2}\right)) \cdot \xi(\bar{\mathbf{o}}_B\!\to\!\mathbf{o}_{B+1}\left(\tfrac{t}{2}\right))^* e^{ik\cdot\Delta_{\mathbf{t}B}\cdot\widehat{\bar{\mathbf{o}}_B\mathbf{o}_{B+1}}}, \qquad (S33)$$

Substituting Eqs. (S30–S33) in Eq. (S29) we get

$$\prod_{b=0}^{B} \xi(\mathbf{o}_b\left(-\tfrac{t}{2}\right)\!\to\!\mathbf{o}_{b+1}\left(-\tfrac{t}{2}\right)) \cdot \xi(\mathbf{o}_b\left(\tfrac{t}{2}\right)\!\to\!\mathbf{o}_{b+1}\left(\tfrac{t}{2}\right))^* \approx$$

$$\xi(\mathbf{o}_0\left(-\tfrac{t}{2}\right)\!\to\!\bar{\mathbf{o}}_1) \cdot \xi(\mathbf{o}_0\left(\tfrac{t}{2}\right)\!\to\!\bar{\mathbf{o}}_1)^*$$

$$\xi(\bar{\mathbf{o}}_B\!\to\!\mathbf{o}_{B+1}\left(-\tfrac{t}{2}\right)) \cdot \xi(\bar{\mathbf{o}}_B\!\to\!\mathbf{o}_{B+1}\left(\tfrac{t}{2}\right))^* \prod_{b=0}^{B} e^{ik(\Delta_{\mathbf{t}b}-\Delta_{\mathbf{t}b+1})\widehat{\bar{\mathbf{o}}_b\bar{\mathbf{o}}_{b+1}}} =$$

$$\xi(\mathbf{o}_0\left(-\tfrac{t}{2}\right)\!\to\!\bar{\mathbf{o}}_1) \cdot \xi(\mathbf{o}_0\left(\tfrac{t}{2}\right)\!\to\!\bar{\mathbf{o}}_1)^*$$

$$\xi(\bar{\mathbf{o}}_B\!\to\!\mathbf{o}_{B+1}\left(-\tfrac{t}{2}\right)) \cdot \xi(\bar{\mathbf{o}}_B\!\to\!\mathbf{o}_{B+1}\left(\tfrac{t}{2}\right))^* \prod_{b=1}^{B} e^{ik\Delta_{\mathbf{t}b}\left(\widehat{\bar{\mathbf{o}}_b\bar{\mathbf{o}}_{b+1}}-\widehat{\bar{\mathbf{o}}_{b-1}\bar{\mathbf{o}}_b}\right)}, \qquad (S34)$$

where $\Delta_{\mathbf{t}0} = \Delta_{\mathbf{t}B+1} = 0$. $\square$

With the help of the above claim we can approximate the path contribution as

$$c_{\vec{\mathbf{x}}^s,\vec{\Delta}_t}\left(-\tfrac{t}{2},\tfrac{t}{2}\right) = \prod_{b=0}^{B} f_b^A, \qquad (S35)$$

with

$$f_b^A = \begin{cases} v(\bar{\mathbf{o}}_2\!\to\!\bar{\mathbf{o}}_1\!\to\!\mathbf{i}_1)\cdot v(\bar{\mathbf{o}}_2\!\to\!\bar{\mathbf{o}}_1\!\to\!\mathbf{i}_2)^*\cdot\sigma_s(\bar{\mathbf{o}}_1), & \text{for } b=0 \\[2em] p(\Delta_{\mathbf{t}1})\cdot e^{ik\left(\widehat{\bar{\mathbf{o}}_1\bar{\mathbf{o}}_2}-1/2(\widehat{\mathbf{i}_1+\mathbf{i}_2}),\bar{\mathbf{o}}_1\right)\cdot\Delta_{\mathbf{t}b}}. \\ \tilde{\alpha}(\bar{\mathbf{o}}_1,\bar{\mathbf{o}}_2)^2\cdot\sigma_s(\bar{\mathbf{o}}_2), & \text{for } b=1 \\[2em] p(\Delta_{\mathbf{t}b})\cdot e^{ik\left(\widehat{\bar{\mathbf{o}}_b\bar{\mathbf{o}}_{b+1}}-\widehat{\bar{\mathbf{o}}_{b-1}\bar{\mathbf{o}}_b}\right)\cdot\Delta_{\mathbf{t}b}}\cdot\rho(\widehat{\bar{\mathbf{o}}_{b-1}\bar{\mathbf{o}}_b}\cdot\widehat{\bar{\mathbf{o}}_b\bar{\mathbf{o}}_{b+1}})\cdot \\ \tilde{\alpha}(\bar{\mathbf{o}}_b,\bar{\mathbf{o}}_{b+1})^2\cdot\sigma_s(\bar{\mathbf{o}}_{b+1}), & \text{for } 2\leq b\leq B-1 \\[2em] p(\Delta_{\mathbf{t}B})\cdot e^{ik\left(\bar{\mathbf{o}}_B,\widehat{1/2(\mathbf{v}_1+\mathbf{v}_2)}-\widehat{\bar{\mathbf{o}}_{B-1}\bar{\mathbf{o}}_B}\right)\cdot\Delta_{\mathbf{t}B}}. \\ v(\bar{\mathbf{o}}_{B-1}\!\to\!\bar{\mathbf{o}}_B\!\to\!\mathbf{v}_1)\cdot v(\bar{\mathbf{o}}_{B-1}\!\to\!\bar{\mathbf{o}}_B\!\to\!\mathbf{v}_2)^*, & \text{for } b=B \end{cases}$$
$$(S36)$$

where we shorten notation by using

$$\tilde{\alpha}(\bar{\mathbf{o}}_b,\bar{\mathbf{o}}_{b+1}) = \frac{1}{r(\bar{\mathbf{o}}_b,\bar{\mathbf{o}}_{b+1})}\alpha(\bar{\mathbf{o}}_b,\bar{\mathbf{o}}_{b+1}). \qquad (S37)$$

In the above formula we could simplify the expression for the central segments ($2 \leq b \leq B-1$) because the same vertices are shared between the paths $\vec{\mathbf{x}}^1, \vec{\mathbf{x}}^2$. For the first and last segments the path segments are different. Eq. (S36) considerably simplifies the path contribution compared to Eq. (S20), but still in order to evaluate the covariance of Eq. (S18) we need to integrate over the space of all sub-paths $\vec{\mathbf{x}}^s$ and all displacement sequences $\vec{\Delta}_t$. Unfortunately, the integration over sub-paths does not lend itself to an analytical solution, and is usually performed using Monte Carlo sampling as we show in the next section. However, assuming the displacements follow a Gaussian distribution as defined in the main paper, we can analytically integrate the space of all displacements for each central subpath.

Claim S3

$$c_{\vec{\mathbf{x}}^s} \equiv \int c_{\vec{\mathbf{x}}^s,\vec{\Delta}_t}\,\mathrm{d}\vec{\Delta}_t = \prod_{b=0}^{B} f_b^I, \qquad (S38)$$

with

$$f_b^I = \begin{cases} v(\bar{\mathbf{o}}_2\!\to\!\bar{\mathbf{o}}_1\!\to\!\mathbf{i}_1)\cdot v(\bar{\mathbf{o}}_2\!\to\!\bar{\mathbf{o}}_1\!\to\!\mathbf{i}_2)^*\cdot\sigma_s(\bar{\mathbf{o}}_1), & \text{for } b=0 \\[2em] \gamma(\widehat{\bar{\mathbf{o}}_1,\bar{\mathbf{o}}_2}-1/2(\widehat{\mathbf{i}_1+\mathbf{i}_2}),\bar{\mathbf{o}}_1)\cdot \\ \tilde{\alpha}(\bar{\mathbf{o}}_1,\bar{\mathbf{o}}_2)^2\cdot\sigma_s(\bar{\mathbf{o}}_2), & \text{for } b=1 \\[2em] \gamma(\widehat{\bar{\mathbf{o}}_b,\bar{\mathbf{o}}_{b+1}}-\widehat{\bar{\mathbf{o}}_{b-1},\bar{\mathbf{o}}_b})\cdot\rho(\widehat{\bar{\mathbf{o}}_{b-1}\bar{\mathbf{o}}_b}\cdot\widehat{\bar{\mathbf{o}}_b\bar{\mathbf{o}}_{b+1}})\cdot \\ \tilde{\alpha}(\bar{\mathbf{o}}_b,\bar{\mathbf{o}}_{b+1})^2\cdot\sigma_s(\bar{\mathbf{o}}_{b+1}) & \text{for } 2\leq b\leq B-1 \\[2em] \gamma(\bar{\mathbf{o}}_B,\widehat{1/2(\mathbf{v}_1+\mathbf{v}_2)}-\widehat{\bar{\mathbf{o}}_{B-1},\bar{\mathbf{o}}_B})\cdot v(\bar{\mathbf{o}}_{B-1}\!\to\!\bar{\mathbf{o}}_B\!\to\!\mathbf{v}_1)\cdot \\ v(\bar{\mathbf{o}}_{B-1}\!\to\!\bar{\mathbf{o}}_B\!\to\!\mathbf{v}_2)^*, & \text{for } b=B \end{cases}$$
$$(S39)$$

with

$$\gamma(\widehat{\bar{\mathbf{o}}_b\bar{\mathbf{o}}_{b+1}}-\widehat{\bar{\mathbf{o}}_{b-1}\bar{\mathbf{o}}_b}) =$$
$$e^{-k^2 D|t|\|\widehat{\bar{\mathbf{o}}_b\bar{\mathbf{o}}_{b+1}}-\widehat{\bar{\mathbf{o}}_{b-1}\bar{\mathbf{o}}_b}\|^2+ikt(\widehat{\bar{\mathbf{o}}_b\bar{\mathbf{o}}_{b+1}}-\widehat{\bar{\mathbf{o}}_{b-1}\bar{\mathbf{o}}_b})\cdot\mathbf{U}}. \qquad (S40)$$

Proof: Our derivation is based on the following integral relation, showing that for any vector $\mathbf{y} \in \mathbb{R}^3$:

$$\mathrm{E}_{\Delta_{\mathbf{t}}}\left[e^{ik\cdot\mathbf{y}\cdot\Delta_{\mathbf{t}}}\right] = \int_{\Delta_{\mathbf{t}}\in\mathbb{R}^3} p(\Delta_{\mathbf{t}})e^{ik\cdot\mathbf{y}\cdot\Delta_{\mathbf{t}}}$$

$$= \int_{\Delta_{\mathbf{t}}\in\mathbb{R}^3} \frac{e^{-\frac{1}{2}(\Delta_{\mathbf{t}}-t\cdot\mathbf{U})^T\Sigma(\Delta_{\mathbf{t}}-t\cdot\mathbf{U})}e^{ik\cdot\mathbf{y}\cdot\Delta_{\mathbf{t}}}}{(2\pi)^{1.5}\det(\Sigma)^{0.5}} \qquad (S41)$$

$$= e^{-k^2 D|t|\cdot\|\mathbf{y}\|^2+ikt\cdot\mathbf{y}\cdot\mathbf{U}}.$$

To compute the desired integral over the displacement sequences of Eq. (S38), we review the original definition of $c_{\vec{\mathbf{x}}^s,\vec{\Delta}_t}$ in Eq. (S35), and note that since the displacement of every node on the path is sampled independently, we can switch between the multiplication and integration operations, and express

$$c_{\vec{\mathbf{x}}^s} = \int c_{\vec{\mathbf{x}}^s,\vec{\Delta}_t}\,\mathrm{d}\vec{\Delta}_t = \int \prod_{b=0}^{B} f_b^A\,\mathrm{d}\vec{\Delta}_t = f_0^A \prod_{b=1}^{B} \int f_b^A\,\mathrm{d}\Delta_{\mathbf{t}b}. \quad (S42)$$

For $2 \leq b \leq B - 1$, we substitute Eq. (S36) in Eq. (S42)

$$
\int f_b^A \, \mathrm{d}\mathbf{\Delta}_{\mathbf{t}b} =
$$
$$
\int p(\mathbf{\Delta}_{\mathbf{t}b}) \cdot e^{ik(\widehat{\bar{\mathbf{o}}_b \bar{\mathbf{o}}_{b+1}} - \widehat{\bar{\mathbf{o}}_{b-1} \bar{\mathbf{o}}_b}) \cdot \mathbf{\Delta}_{\mathbf{t}b}} \cdot
$$
$$
\rho(\widehat{\bar{\mathbf{o}}_{b-1} \bar{\mathbf{o}}_b} \cdot \widehat{\bar{\mathbf{o}}_b \bar{\mathbf{o}}_{b+1}}) \cdot \tilde{\alpha}(\bar{\mathbf{o}}_b, \bar{\mathbf{o}}_{b+1})^2 \cdot \sigma_s(\bar{\mathbf{o}}_{b+1}) \, \mathrm{d}\mathbf{\Delta}_{\mathbf{t}b} =
$$
$$
\rho(\widehat{\bar{\mathbf{o}}_{b-1} \bar{\mathbf{o}}_b} \cdot \widehat{\bar{\mathbf{o}}_b \bar{\mathbf{o}}_{b+1}}) \cdot \tilde{\alpha}(\bar{\mathbf{o}}_b, \bar{\mathbf{o}}_{b+1})^2 \cdot \sigma_s(\bar{\mathbf{o}}_{b+1}) \cdot \qquad \text{(S43)}
$$
$$
\int p(\mathbf{\Delta}_{\mathbf{t}b}) \cdot e^{ik(\widehat{\bar{\mathbf{o}}_b \bar{\mathbf{o}}_{b+1}} - \widehat{\bar{\mathbf{o}}_{b-1} \bar{\mathbf{o}}_b}) \cdot \mathbf{\Delta}_{\mathbf{t}b}} \, \mathrm{d}\mathbf{\Delta}_{\mathbf{t}b} =
$$
$$
\rho(\widehat{\bar{\mathbf{o}}_{b-1} \bar{\mathbf{o}}_b} \cdot \widehat{\bar{\mathbf{o}}_b \bar{\mathbf{o}}_{b+1}}) \cdot \tilde{\alpha}(\bar{\mathbf{o}}_b, \bar{\mathbf{o}}_{b+1})^2 \cdot \sigma_s(\bar{\mathbf{o}}_{b+1}) \cdot
$$
$$
e^{-k^2 D|t| \cdot \|(\widehat{\bar{\mathbf{o}}_b \bar{\mathbf{o}}_{b+1}} - \widehat{\bar{\mathbf{o}}_{b-1} \bar{\mathbf{o}}_b})\|^2 + ikt \cdot (\widehat{\bar{\mathbf{o}}_b \bar{\mathbf{o}}_{b+1}} - \widehat{\bar{\mathbf{o}}_{b-1} \bar{\mathbf{o}}_b}) \cdot \mathbf{U}} =
$$
$$
f_b^I,
$$

where the integral is solved according to Eq. (S41) for $\mathbf{y} = \widehat{\bar{\mathbf{o}}_b \bar{\mathbf{o}}_{b+1}} - \widehat{\bar{\mathbf{o}}_{b-1} \bar{\mathbf{o}}_b}$. Similarly, we get

$$
\int f_1^A \, \mathrm{d}\mathbf{\Delta}_{\mathbf{t}1} = f_1^I, \quad \int f_B^A \, \mathrm{d}\mathbf{\Delta}_{\mathbf{t}B} = f_B^I, \qquad \text{(S44)}
$$

and by setting $f_0^I = f_0^A$, we get

$$
c_{\vec{\mathbf{x}}^s} = f_0^I \prod_{b=1}^B f_b^I = \prod_{b=0}^B f_b^I. \qquad \text{(S45)}
$$

□

Following Claim S3 we can express the covariance as the integral over the space $\mathbb{P}$ of *static* subpaths $\vec{\mathbf{x}}^s$

$$
C_{\mathbf{v}_1, \mathbf{v}_2}^{\mathbf{i}_1, \mathbf{i}_2} \left(-\tfrac{t}{2}, \tfrac{t}{2}\right) = \int_{\mathbb{P}} c_{\vec{\mathbf{x}}^s} \left(-\tfrac{t}{2}, \tfrac{t}{2}\right) \, \mathrm{d}\vec{\mathbf{x}}^s \qquad \text{(S46)}
$$

where the average contribution of all pairs of paths sharing vertices $\mathbf{o}_1, \ldots, \mathbf{o}_B$ is

$$
c_{\vec{\mathbf{x}}^s} \left(-\tfrac{t}{2}, \tfrac{t}{2}\right) = \prod_{b=0}^B f_b^I \qquad \text{(S47)}
$$

2. ESTIMATING SPECKLE COVARIANCES

We include here the complete Monte Carlo sampling algorithm that estimates the speckle covariances. This follows the derivation in the main text, along with accurate handling of special cases, such as paths of length 1, and absorption. In Alg. S1 we consider homogeneous volumes with uniform material density, in which case sampling from $\alpha(\bar{\mathbf{o}}_{b-1}, \bar{\mathbf{o}}_b)^2 \cdot \sigma_s(\bar{\mathbf{o}}_b)$ reduces to a straightforward sampling from an exponential distribution. For heterogeneous, spatially varying densities one should sample using a Woodcock tracking scheme [4], as described in Alg. S2.

In Fig. S4 we perform an equal-sample comparison of path tracing algorithms with and without next-event estimation. When next-event estimation is used one can use an infinitesimally small sensor. Without this, the quality of the estimate is largely dependent on the size of the sensor used in the simulation, where with wider sensors the probability that paths will reach the sensor is higher, and hence estimation noise decreases. We run each MC simulation for 1000 times using 5×10^7 samples (where a path of length B is counted as B samples), and in Fig. S4 we plot the mean and variance of the different experiments. The simulation considers temporal-only correlations, where path-tracing without next-event estimation uses the MCX implementation [5], and next-event estimation uses our

---

Algorithm S1: Monte Carlo covariance rendering for homogeneous volumes.

> *Initialize covariance estimate.*
Set $C = 0$.
for *iteration* $= 1 : N$ **do**
    ▷ *Sample a subpath:*
    ▷ *Sample first vertex.*
    Sample point $\bar{\mathbf{o}}_1$ with the probability $q_1(\bar{\mathbf{o}}_1)$.
    ▷ *Update covariance with single scattering path.*
    Update $C \mathrel{+}= \frac{1}{q_1(\bar{\mathbf{o}}_1)} \gamma(\bar{\mathbf{o}}_1, \tfrac{1}{2}\widehat{(\mathbf{v}_1 + \mathbf{v}_2)} - \tfrac{1}{2}\widehat{(\mathbf{i}_1 + \mathbf{i}_2)}, \bar{\mathbf{o}}_1) \cdot$
       $v(\mathbf{v}_1 \rightarrow \bar{\mathbf{o}}_1 \rightarrow \mathbf{i}_1) \cdot v(\mathbf{v}_2 \rightarrow \bar{\mathbf{o}}_1 \rightarrow \mathbf{i}_2)^* \cdot \sigma_s$.
    ▷ *Continue tracing the subpath.*
    ▷ *Sample first direction.*
    Sample direction $\hat{\boldsymbol{\omega}}_1$ and compute the probability $q_1(\bar{\mathbf{o}}_1, \hat{\boldsymbol{\omega}}_1)$.
    ▷ *Sample second vertex of subpath.*
    Sample distance $d \sim \sigma_t e^{-\sigma_t d}$.
    Set point $\bar{\mathbf{o}}_2 = \bar{\mathbf{o}}_1 + d \cdot \hat{\boldsymbol{\omega}}_1$.
    Set $b = 2$.
    Set $f_0^I = v(\bar{\mathbf{o}}_2 \rightarrow \bar{\mathbf{o}}_1 \rightarrow \mathbf{i}_1) \cdot v(\bar{\mathbf{o}}_2 \rightarrow \bar{\mathbf{o}}_1 \rightarrow \mathbf{i}_2)^* \cdot \sigma_s(\bar{\mathbf{o}}_1)$.
    Set $\gamma_0 = \gamma(\widehat{\bar{\mathbf{o}}_1, \bar{\mathbf{o}}_2} - \tfrac{1}{2}\widehat{(\mathbf{i}_1 + \mathbf{i}_2)}, \bar{\mathbf{o}}_1)$.
    Set $\gamma_1 = \gamma_2 = 1$.
    while $\bar{\mathbf{o}}_b$ *inside medium* **do**
       ▷ *Account for absorption.*
       Sample scalar $a \sim \mathrm{Unif}[0, 1]$.
       if $a > \sigma_s/\sigma_t$ **then**
          ▷ *Terminate subpath at absorption event.*
          break
       end
       if $b \geq 3$ **then**
          ▷ *Update momentum transfer.*
          $\gamma_b = \gamma_{b-1} \cdot \gamma(\widehat{\bar{\mathbf{o}}_{b-1} \bar{\mathbf{o}}_b} - \widehat{\bar{\mathbf{o}}_{b-2} \bar{\mathbf{o}}_{b-1}})$.
       end
       ▷ *Update covariance with next-event estimation.*
       Set $\gamma_B = \gamma(\bar{\mathbf{o}}_b, \tfrac{1}{2}\widehat{(\mathbf{v}_1 + \mathbf{v}_2)} - \widehat{\bar{\mathbf{o}}_{b-1}, \bar{\mathbf{o}}_b})$.
       Set $f_B^I = \gamma_B \cdot v(\bar{\mathbf{o}}_{b-1} \rightarrow \bar{\mathbf{o}}_b \rightarrow \mathbf{v}_1) \cdot v(\bar{\mathbf{o}}_{b-1} \rightarrow \bar{\mathbf{o}}_b \rightarrow \mathbf{v}_2)^*$.
       Update $C \mathrel{+}= \frac{1}{q_1(\bar{\mathbf{o}}_1, \hat{\boldsymbol{\omega}}_1)} \cdot f_0^I \cdot \gamma_0 \cdot f_B^I \cdot \gamma_{b-1}$.
       ▷ *Sample next vertex of subpath.*
       ▷ *Sample direction from phase function.*
       Sample direction $\hat{\boldsymbol{\omega}}_b \sim \rho(\hat{\boldsymbol{\omega}}_{b-1} \cdot \hat{\boldsymbol{\omega}}_b)$.
       ▷ *Sample free path.*
       Sample distance $d \sim \sigma_t e^{-\sigma_t d}$.
       ▷ *Create next vertex of subpath.*
       Set point $\bar{\mathbf{o}}_{b+1} = \bar{\mathbf{o}}_b + d \cdot \hat{\boldsymbol{\omega}}_b$.
       Set $b = b + 1$.
    end
end
> *Produce final covariance estimate.*
Update $C = \frac{1}{N} C$.
return C.

---

own implementation. While the mean of all approaches agree, without next-event estimation small sensors exhibit very large noise variance. This noise reduces with wider sensors.

At the moment our proof of concept implementation is not as fast as MCX [5]. We hope that some of the ideas introduced for temporal-only MC [6–8], as well as incoherent path tracing ideas developed in computer graphics [9–11] can be incorporated into a fully efficient spatio-temporal Monte Carlo simulator.

3. SAMPLING A SPECKLE FIELD

In this section we formally prove that fields sampled using our approach have the desired covariance. As mentioned in the main paper, we assume we are given a list of J sources $\mathbf{i}_1, \ldots, \mathbf{i}_J$, sensors $\mathbf{v}_1, \ldots, \mathbf{v}_J$, and time indices $t_1, \ldots, t_J$, and wish to sample J complex numbers $u_{\mathbf{v}_1}^{\mathbf{i}_1}, \ldots, u_{\mathbf{v}_J}^{\mathbf{i}_J}$ that have the same covariance as computed by the MC algorithm that computes covariances

Algorithm S2: Monte Carlo covariance rendering for heterogeneous volumes.

> ▷Initialize covariance estimate.

Set $C = 0$.
Set $\sigma_{t,\max} = \max \sigma_t(\mathbf{o})$
for iteration $= 1 : N$ **do**
    ▷Sample a subpath:
    ▷Sample first vertex.
    Sample point $\bar{\mathbf{o}}_1$ with the probability $q_1(\bar{\mathbf{o}}_1)$.
    ▷Update covariance with single scattering path.
    Update $C \mathrel{+}= \frac{1}{q_1(\bar{\mathbf{o}}_1)} \gamma(\bar{\mathbf{o}}_1, \widehat{1/2(\mathbf{v}_1 + \mathbf{v}_2)} - \widehat{1/2(\mathbf{i}_1 + \mathbf{i}_2)}, \bar{\mathbf{o}}_1) \cdot$
        $v(\mathbf{v}_1 \to \bar{\mathbf{o}}_1 \to \mathbf{i}_1) \cdot v(\mathbf{v}_2 \to \bar{\mathbf{o}}_1 \to \mathbf{i}_2)^* \cdot \sigma_s(\bar{\mathbf{o}}_1)$.
    ▷Continue tracing the subpath.
    ▷Sample first direction.
    Sample direction $\hat{\boldsymbol{\omega}}_1$ and compute the probability $q_1(\bar{\mathbf{o}}_1, \hat{\boldsymbol{\omega}}_1)$.
    Set $b = 2$.
    Set $f_0^I = v(\bar{\mathbf{o}}_2 \to \bar{\mathbf{o}}_1 \to \mathbf{i}_1) \cdot v(\bar{\mathbf{o}}_2 \to \bar{\mathbf{o}}_1 \to \mathbf{i}_2)^* \cdot \sigma_s(\bar{\mathbf{o}}_1)$.
    Set $\gamma_0 = \gamma(\widehat{\bar{\mathbf{o}}_1, \bar{\mathbf{o}}_2} - \widehat{1/2(\mathbf{i}_1 + \mathbf{i}_2)}, \bar{\mathbf{o}}_1)$.
    Set $\gamma_1 = \gamma_2 = 1$.
    do
        ▷Perform Woodcock tracking step for next vertex of subpath.
        Set $d = 0$.
        do
            Sample scalars $\chi_1 \sim \text{Unif}[0,1]$, $\chi_2 \sim \text{Unif}[0,1]$.
            $d \mathrel{+}= -\log(\chi_1 + 1)/\sigma_{t,\max}$.
            Set point $\bar{\mathbf{o}}_b = \bar{\mathbf{o}}_{b-1} + d \cdot \hat{\boldsymbol{\omega}}_{b-1}$.
        while $\bar{\mathbf{o}}_b$ inside medium **or** $\chi_2 \leq \sigma_t(\bar{\mathbf{o}}_b)/\sigma_{t,\max}$;
        ▷Account for absorption.
        Sample scalar $a \sim \text{Unif}[0,1]$.
        if $a > \sigma_s(\bar{\mathbf{o}}_b)/\sigma_t(\bar{\mathbf{o}}_b)$ **or** $\bar{\mathbf{o}}_b$ outside medium **then**
            ▷Terminate subpath.
            break
        end
        if $b \geq 3$ **then**
            ▷Update momentum transfer.
            $\gamma_b = \gamma_{b-1} \cdot \gamma(\widehat{\bar{\mathbf{o}}_{b-1} \bar{\mathbf{o}}_b} - \widehat{\bar{\mathbf{o}}_{b-2} \bar{\mathbf{o}}_{b-1}})$.
        end
        ▷Update covariance with next-event estimation.
        Set $\gamma_B = \gamma(\bar{\mathbf{o}}_b, \widehat{1/2(\mathbf{v}_1 + \mathbf{v}_2)} - \widehat{\bar{\mathbf{o}}_{b-1} \bar{\mathbf{o}}_b})$.
        Set $f_B^I = \gamma_B \cdot v(\bar{\mathbf{o}}_{b-1} \to \bar{\mathbf{o}}_b \to \mathbf{v}_1) \cdot v(\bar{\mathbf{o}}_{b-1} \to \bar{\mathbf{o}}_b \to \mathbf{v}_2)^*$.
        Update $C \mathrel{+}= \frac{1}{q_1(\bar{\mathbf{o}}_1, \hat{\boldsymbol{\omega}}_1)} \cdot f_0^I \cdot \gamma_0 \cdot f_B^I \cdot \gamma_{b-1}$.
        ▷Sample direction from phase function at $\bar{\mathbf{o}}_b$.
        Sample direction $\hat{\boldsymbol{\omega}}_b \sim \rho(\hat{\boldsymbol{\omega}}_{b-1} \cdot \hat{\boldsymbol{\omega}}_b; \bar{\mathbf{o}}_b)$.
        Set $b = b + 1$.
    while true;
end
▷Produce final covariance estimate.
Update $C = \frac{1}{N} C$.
return C.

directly. That is, for every j, k,

$$\mathrm{E}\left[u_{\mathbf{v}_j}^{\mathbf{i}_j} \cdot u_{\mathbf{v}_k}^{\mathbf{i}_k *}\right] - \mathrm{E}\left[u_{\mathbf{v}_j}^{\mathbf{i}_j}\right] \cdot \mathrm{E}\left[u_{\mathbf{v}_k}^{\mathbf{i}_k}\right]^* = C_{\mathbf{v}_j, \mathbf{v}_k}^{\mathbf{i}_j, \mathbf{i}_k}(t_j, t_k) \quad \text{(S48)}$$

To do this we sample N subpaths $\vec{\mathbf{x}}^{s,n}$. For each subpath we

Algorithm S3: Sampling temporal displacements

Set $\boldsymbol{\Delta}_{t_1} = \mathbf{0}$.
for $j = 2 : J$ **do**
    Set $dt = t_j - t_{j-1}$.
    Sample a 3D vector $\mathbf{w}$ from a unit normal distribution.
    Set $\boldsymbol{\Delta}_{dt} = \sqrt{2 \cdot D |dt|} \cdot \mathbf{w} + dt \cdot \mathbf{U}$.
    Set $\boldsymbol{\Delta}_{t_j} = \boldsymbol{\Delta}_{t_{j-1}} + \boldsymbol{\Delta}_{dt}$.
end
Set $\forall j, \mathbf{o}(t_j) = \bar{\mathbf{o}} - \boldsymbol{\Delta}_0 + \boldsymbol{\Delta}_{t_j}$.
return $\{\mathbf{o}(t_j)\}_{j=1}^J$.

sample a sequence of temporal displacements $\vec{\boldsymbol{\Delta}}_{t_j}^n$ from $\mathcal{T}$. We
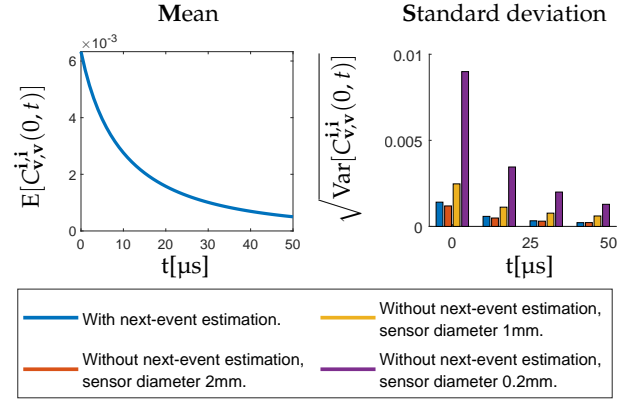
Fig. S4. An equal-sample comparison of path tracing algorithms with and without next-event estimation. We compute temporal-only correlations ($C_{\mathbf{v},\mathbf{v}}^{\mathbf{i},\mathbf{i}}(0,t)$) with both approaches and plot the mean and variance. While at the limit of many samples all algorithms produce the same correlation, when each algorithm is run for 5×10^7 samples only, the estimation of small sensors without next-event estimation is very noisy. This noise reduces when we increase sensor size. Next-event estimation can simulate infinitesimally small sensors. The simulation uses the parameters of Fig. 5(b) from the main paper, $\delta = 2$ cm.

define $N \times J$ paths

$$\vec{\mathbf{x}}_j^n(t_j) = \mathbf{i}_j \to \vec{\mathbf{x}}^{s,n} + \vec{\boldsymbol{\Delta}}_{t_j}^n \to \mathbf{v}_j \quad \text{(S49)}$$

We define the sampled fields as the sum of contributions from these paths. Each path has a phase proportional to its length and we also need to take into account the attenuation and scattering amplitude function at the first and last segments, as those are not sampled by q. This leads to the fields

$$u_{\mathbf{v}_j}^{\mathbf{i}_j} = \frac{1}{N} \sum_{n=1}^N u_{\mathbf{v}_j}^{n,\mathbf{i}_j} \quad \text{(S50)}$$

with

$$u_{\mathbf{v}_j}^{n,\mathbf{i}_j} = \sqrt{\frac{\sigma_s(\bar{\mathbf{o}}_1^n)}{q_1(\bar{\mathbf{o}}_1^n, \hat{\boldsymbol{\omega}}_1^n)}} s(\widehat{\mathbf{i}_j, \bar{\mathbf{o}}_1^n} \cdot \widehat{\bar{\mathbf{o}}_1^n, \bar{\mathbf{o}}_2^n}) \cdot s(\widehat{\bar{\mathbf{o}}_{B-1}^n, \bar{\mathbf{o}}_B^n} \cdot \widehat{\bar{\mathbf{o}}_B^n, \mathbf{v}_j})$$
$$\cdot \tilde{\alpha}(\mathbf{i}_j, \bar{\mathbf{o}}_1^n) \cdot \tilde{\alpha}(\bar{\mathbf{o}}_B^n, \mathbf{v}_j) \prod_{b=0}^B \xi(\mathbf{o}_b^n(t_j) \to \mathbf{o}_{b+1}^n(t_j)) \quad \text{(S51)}$$

The displacement sampling algorithm is described in Alg. S3. Without the loss of generality, we assume that $\{t_j\}_{j=1}^J$ is a non-decreasing sequence. The homogeneous and heterogeneous versions of the field sampling algorithm are summarized in Algs. S4 and S5, along with a more detailed handling of special cases such as paths of length 1.

Claim S4 *For zero-mean fields where $m_{\mathbf{v}^j}^{\mathbf{i}^j} = 0$, the rendering strategy of Eq. (S50) follows the covariance*

$$C_{\mathbf{v}_j, \mathbf{v}_k}^{\mathbf{i}_j, \mathbf{i}_k}\left(-\tfrac{t}{2}, \tfrac{t}{2}\right) = \int_{\mathbb{P}} c_{\vec{\mathbf{x}}^s}\left(-\tfrac{t}{2}, \tfrac{t}{2}\right) d\vec{\mathbf{x}}^s \quad \text{(S52)}$$

Proof: We provide the proof assuming we attempt to sample zero-mean fields $\mathrm{E}[u_{\mathbf{v}_j}^{\mathbf{i}_j}] = 0$. As the different paths are sampled

---

Algorithm S4: Monte Carlo field rendering for homogeneous volumes .

▷*Initialize field estimate.*
Set $\mathbf{u} = \mathbf{0}$.
for *iteration* $= 1 : N$ **do**
 Sample random phase $\zeta \sim \mathrm{Unif}[0,1]$.
 Set $z = e^{2\pi i \zeta}$.
  ▷*Sample first vertex of subpath.*
 Sample point $\bar{\mathbf{o}}_1$ with the probability $q_1(\bar{\mathbf{o}}_1)$.
  ▷*Sample temporal displacements.*
 $\{\mathbf{o}_1(t_j)\}_{j=1}^J = \mathrm{TemporalDisplacement}(\bar{\mathbf{o}}_1)$.
  ▷*Update field with single scattering path.*
 Update $\forall j, \mathbf{u}_j \mathrel{+}= z \cdot \sqrt{\frac{\sigma_s(\mathbf{o}_1(t_j))}{q_1(\bar{\mathbf{o}}_1)}} \cdot$
  $v(\mathbf{i}_j \to \mathbf{o}_1(t_j)) v(\mathbf{i}_j \to \mathbf{o}_1(t_j) \to \mathbf{v}_j)$.
   ▷*Continue tracing the subpath.*
   ▷*Sample first direction.*
 Sample direction $\hat{\omega}_1$ and compute the probability $q_1(\bar{\mathbf{o}}_1, \hat{\omega}_1)$.
  ▷*Sample second vertex of subpath.*
 Sample distance $d \sim \sigma_t e^{-\sigma_t d}$.
 Set point $\bar{\mathbf{o}}_2 = \bar{\mathbf{o}}_1 + d \cdot \hat{\omega}_1$.
 Set $b = 2$.
 Set $\forall j, \delta_j = 0$.
 while $\bar{\mathbf{o}}_b$ *inside medium* **do**
   ▷*Account for absorption.*
  Sample scalar $a \sim \mathrm{Unif}[0,1]$.
  if $a > \sigma_s/\sigma_t$ **then**
    ▷*Terminate subpath at absorption event.*
   break
  end
    ▷*Sample temporal displacements.*
  $\{\mathbf{o}_b(t_j)\}_{j=1}^J = \mathrm{TemporalDisplacement}(\bar{\mathbf{o}}_b)$.
  Update $\forall j, \delta_j \mathrel{+}= |\mathbf{o}_b(t_j) - \mathbf{o}_{b-1}(t_j)|$.
  Sample random phase $\zeta \sim \mathrm{Unif}[0,1]$.
  Set $\forall j, z_j = e^{2\pi i \zeta + k i \delta_j}$.
    ▷*Update field with next-event estimation.*
  Update $\forall j, \mathbf{u}_j \mathrel{+}= z_j \cdot \sqrt{\frac{\sigma_s(\mathbf{o}_b(t_j))}{q_1(\bar{\mathbf{o}}_1, \hat{\omega}_1)}} \cdot$
  $v(\mathbf{o}_2(t_j)) \to \mathbf{o}_1(t_j)) \to \mathbf{i}_j) v(\mathbf{o}_{b-1}(t_j) \to \mathbf{o}_b(t_j) \to \mathbf{v}_j)$
    ▷*Sample next vertex of subpath.*
    ▷*Sample direction from phase function.*
  Sample direction $\hat{\omega}_b \sim \rho(\hat{\omega}_{b-1} \cdot \hat{\omega}_b)$.
    ▷*Sample free path.*
  Sample distance $d \sim \sigma_t e^{-\sigma_t d}$.
    ▷*Create next vertex of subpath.*
  Set point $\bar{\mathbf{o}}_{b+1} = \bar{\mathbf{o}}_b + d \cdot \hat{\omega}_b$.
  Set $b = b + 1$.
 end
end
  ▷*Produce final field with correct mean.*
Update $\forall j, \mathbf{u}_j = m_{\mathbf{v}_j}^{\mathbf{i}_j} + \sqrt{\frac{1}{N}} \mathbf{u}_j$.
return $\mathbf{u}$.

Algorithm S5: Monte Carlo field rendering for heterogeneous volumes.

▷*Initialize field estimate.*
Set $\mathbf{u} = \mathbf{0}$.
Set $\sigma_{t,\max} = \max \sigma_t(\mathbf{o})$
for *iteration* $= 1 : N$ **do**
 Sample random phase $\zeta \sim \mathrm{Unif}[0,1]$.
 Set $z = e^{2\pi i \zeta}$.
  ▷*Sample first vertex of subpath.*
 Sample point $\bar{\mathbf{o}}_1$ with the probability $q_1(\bar{\mathbf{o}}_1)$.
  ▷*Sample temporal displacements.*
 $\{\mathbf{o}_1(t_j)\}_{j=1}^J = \mathrm{TemporalDisplacement}(\bar{\mathbf{o}}_1)$.
  ▷*Update field with single scattering path.*
 Update $\forall j, \mathbf{u}_j \mathrel{+}= z \cdot \sqrt{\frac{\sigma_s(\mathbf{o}_1(t_j))}{q_1(\bar{\mathbf{o}}_1)}} \cdot$
  $v(\mathbf{i}_j \to \mathbf{o}_1(t_j)) v(\mathbf{i}_j \to \mathbf{o}_1(t_j) \to \mathbf{v}_j)$.
   ▷*Continue tracing the subpath.*
   ▷*Sample first direction.*
 Sample direction $\hat{\omega}_1$ and compute the probability $q_1(\bar{\mathbf{o}}_1, \hat{\omega}_1)$.
 Set $b = 2$.
 Set $\forall j, \delta_j = 0$.
 do
   ▷*Perform Woodcock tracking step for next vertex of subpath.*
  Set $d = 0$.
  do
   Sample scalars $\chi_1 \sim \mathrm{Unif}[0,1], \chi_2 \sim \mathrm{Unif}[0,1]$.
   $d \mathrel{+}= -\log(\chi_1 + 1)/\sigma_{t,\max}$.
   Set point $\bar{\mathbf{o}}_b = \bar{\mathbf{o}}_{b-1} + d \cdot \hat{\omega}_{b-1}$.
  while $\bar{\mathbf{o}}_b$ *inside medium or* $\chi_2 \le \sigma_t(\bar{\mathbf{o}}_b)/\sigma_{t,\max}$;
    ▷*Account for absorption.*
  Sample scalar $a \sim \mathrm{Unif}[0,1]$.
  if $a > \sigma_s(\bar{\mathbf{o}}_b)/\sigma_t(\bar{\mathbf{o}}_b)$ *or* $\bar{\mathbf{o}}_b$ *outside medium* **then**
    ▷*Terminate subpath.*
   break
  end
    ▷*Sample temporal displacements.*
  $\{\mathbf{o}_b(t_j)\}_{j=1}^J = \mathrm{TemporalDisplacement}(\bar{\mathbf{o}}_b)$.
  Update $\forall j, \delta_j \mathrel{+}= |\mathbf{o}_b(t_j) - \mathbf{o}_{b-1}(t_j)|$.
  Sample random phase $\zeta \sim \mathrm{Unif}[0,1]$.
  Set $\forall j, z_j = e^{2\pi i \zeta + k i \delta_j}$.
    ▷*Update field with next-event estimation.*
  Update $\forall j, \mathbf{u}_j \mathrel{+}= z_j \cdot \sqrt{\frac{\sigma_s(\mathbf{o}_b(t_j))}{q_1(\bar{\mathbf{o}}_1, \hat{\omega}_1)}} \cdot$
  $v(\mathbf{o}_2(t_j)) \to \mathbf{o}_1(t_j)) \to \mathbf{i}_j) v(\mathbf{o}_{b-1}(t_j) \to \mathbf{o}_b(t_j) \to \mathbf{v}_j)$
    ▷*Sample direction from phase function.*
  Sample direction $\hat{\omega}_b \sim \rho(\hat{\omega}_{b-1} \cdot \hat{\omega}_b; \bar{\mathbf{o}}_b)$.
  Set $b = b + 1$.
 while *true*;
end
  ▷*Produce final field with correct mean.*
Update $\forall j, \mathbf{u}_j = m_{\mathbf{v}_j}^{\mathbf{i}_j} + \sqrt{\frac{1}{N}} \mathbf{u}_j$.
return $\mathbf{u}$.

---

independently there is no correlation between the contribution of different paths $u_{\mathbf{v}_j}^{n,\mathbf{i}_j}$, and we can express

$$\mathrm{E}\left[u_{\mathbf{v}_j}^{\mathbf{i}_j} \cdot u_{\mathbf{v}_k}^{\mathbf{i}_k *}\right] = \mathrm{E}\left[\frac{1}{N^2} \sum_n u_{\mathbf{v}_j}^{n,\mathbf{i}_j} \cdot \sum_n u_{\mathbf{v}_k}^{n,\mathbf{i}_k *}\right]$$

$$= \mathrm{E}\left[u_{\mathbf{v}_j}^{n,\mathbf{i}_j} \cdot u_{\mathbf{v}_k}^{n,\mathbf{i}_k *}\right]. \tag{S53}$$

The expectation can be expressed as the integral over the path sampling probability q

$$\int_{\vec{\mathbf{x}}^{s,n}, \vec{\mathbf{\Delta}}_{t_j}} q(\vec{\mathbf{x}}^{s,n}) p(\vec{\mathbf{\Delta}}_{t_j}, \vec{\mathbf{\Delta}}_{t_k}) u_{\mathbf{v}_j}^{n,\mathbf{i}_j} \cdot u_{\mathbf{v}_k}^{n,\mathbf{i}_k *} \tag{S54}$$

with

$$q(\bar{\mathbf{o}}_b) = \tilde{\alpha}(\bar{\mathbf{o}}_{b-1}, \bar{\mathbf{o}}_b)^2 \cdot \sigma_s(\bar{\mathbf{o}}_b). \tag{S55}$$

$$q(\hat{\omega}_b | \bar{\mathbf{o}}_b) = \rho(\widehat{\bar{\mathbf{o}}_{b-1}\bar{\mathbf{o}}_b} \cdot \widehat{\bar{\mathbf{o}}_b\bar{\mathbf{o}}_{b+1}}). \tag{S56}$$

Substituting the path sampling distribution q defined by Eq. (S55) and Eq. (S56) as well as Claim S2, we get that the above expectation reduces to

$$\int_{\vec{\mathbf{x}}^{s,n}, \vec{\mathbf{\Delta}}_{t_j}} p(\vec{\mathbf{\Delta}}_{t_j}, \vec{\mathbf{\Delta}}_{t_k}) \prod_{b=0}^B f_b^A \tag{S57}$$

as defined in Eq. (S36). Following Claim S3 the integration over displacements results in the terms f_b^I from Eq. (S39), and we end with the desired covariance of Eq. (S52). ☐ So far we have only considered zero-mean fields where $m_{\mathbf{v}_j}^{\mathbf{i}_j} = 0$. This is usually the case as the field is a complex number. The only exception is when the sensor $\mathbf{v}_j$ accumulates some ballistic light

from $\mathbf{i}_j$. In Alg. S4 we ensure the fields we sample are zero mean by sampling a complex phase at every scattering event. This does not change the covariance as the same random phase is added both to $\vec{\mathbf{x}}^{n,j}$ and $\vec{\mathbf{x}}^{n,k}$. After averaging all paths we add the desired mean $m_{\mathbf{v}_j}^{\mathbf{i}_j}$, which can be computed in closed form as explained above.

Fig. S5 simulates a few speckle fields sampled using this algorithm, while varying a few material parameters.

REFERENCES

1. V. Twersky, "On propagation in random media of discrete scatterers," Proc. Symp. Appl. Math (1964).
2. A. Ishimaru, *Wave propagation and scattering in random media*, vol. 12 (John Wiley & Sons, 1999).
3. M. Mishchenko, L. Travis, and A. Lacis, *Multiple scattering of light by particles: radiative transfer and coherent backscattering* (Cambridge University, 2006).
4. P. Kutz, R. Habel, Y. K. Li, and J. Novák, "Spectral and decomposition tracking for rendering heterogeneous volumes," ACM Trans. on Graph. (TOG) (2017).
5. Q. Fang and D. A. Boas, "Monte Carlo simulation of photon migration in 3D turbid media accelerated by graphics processing units," Opt. Express (2009).
6. D. D. Postnov, J. Tang, S. E. Erdener, K. Kılıç, and D. A. Boas, "Dynamic light scattering imaging," Sci. Adv. (2020).
7. S. Xu, X. Yang, W. Liu, J. Jönsson, R. Qian, P. C. Konda, K. C. Zhou, L. Kreiß, H. Wang, Q. Dai, E. Berrocal, and R. Horstmeyer, "Imaging dynamics beneath turbid media via parallelized single-photon detection," Adv. Sci. (2022).
8. B. Lee, O. Sosnovtseva, C. M. Sørensen, and D. D. Postnov, "Multi-scale laser speckle contrast imaging of microcirculatory vasoreactivity," Biomed. Opt. Express (2022).
9. P. Dutre, K. Bala, and P. Bekaert, *Advanced Global Illumination* (A K Peters, Natick, MA, 2006).
10. J. Novak, I. Georgiev, J. Hanika, and W. Jarosz, "Monte Carlo methods for volumetric light transport simulation," Comput. Graph. Forum (2018).
11. E. Veach, "Robust Monte Carlo methods for light transport simulation," Ph.D. thesis, Stanford Uni. (1997).
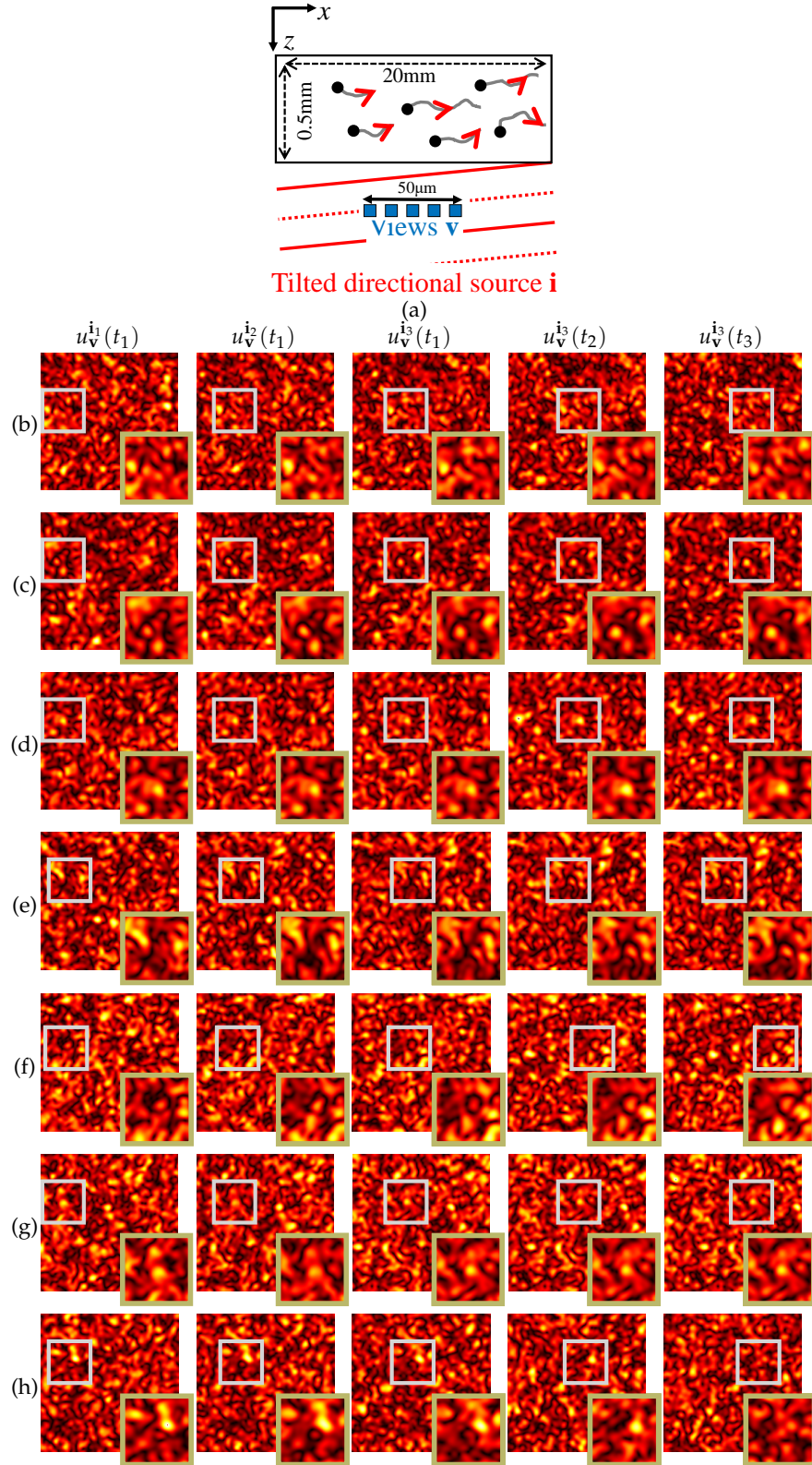
Fig. S5. Sampling speckle images: we use Alg. S4 to sample speckle images with consistent spatio-temporal variations. We demonstrate three speckle images under different illumination directions. Note how the speckle shift with illumination angle, demonstrating memory effect correlations. In subsequent columns the illumination is fixed and we visualize temporal variation of the speckle pattern. In our simulation the volume is illuminated by a plane wave starting at $\hat{\mathbf{i}}_1 = 0°$ and tilting at angular intervals of $0.007°$. The simulated motion includes a mixture of linear and Brownian components with $\mathbf{U}_x = 25$ cm/s, $D = 2 \times 10^{-8}$ cm^2/s, temporal images are sampled at intervals of 25 μs. Particles have MFP = 250 μm and isotropic scattering ($g = 0$). The different rows repeat this simulation while varying the following parameters. (b) MFP = 150 μm, (c) MFP = 500 μm, (d) $g = 0.9$, (e) $\mathbf{U}_x = 0$, (f) $\mathbf{U}_x = 40$ cm/s, (g) $D = 0$, (h) $D = 10 \times 10^{-8}$ cm^2/s